Advances in Atmospheric Correction of Satellite Ocean-Color Imagery: Sun Glint, Thin Clouds, and Adjacency Effects

Robert Frouin
Scripps Institution of Oceanography
University of California San Diego
La Jolla, California

IOCS Meeting, 6-8 May 2013, Darmstadt

With Contributions from

Roland Doerffer, Helmholtz Zentrum Geesthacht,
Institute of Coastal Research, Germany

Lydwine Gross, Capgemini, France

François Steinmetz, HYGEOS, France

Some Facts

1. The inverse ocean-color problem is ill-posed.

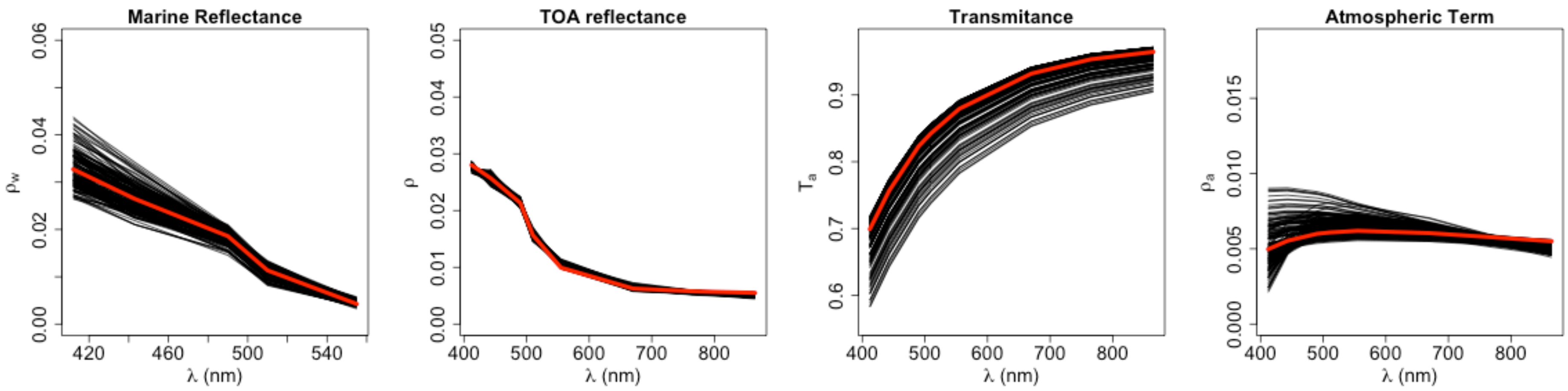

Example of pre-images. Actual values of ρ_w , ρ, T_a, and ρ_a are displayed in red, and the pre-images at a distance no more than δ= 0.001 are displayed in black. The search spaces for the pre-images include NOMAD and AERONET-OC data sets and maritime, continental, and urban aerosols in various proportions and amount.

2. Measurements in two spectral bands in the red, near-infrared, and/or short-wave infrared are not sufficient, in the general case, to determine the perturbing effects of the atmosphere and surface in the visible.

-No sensitivity to aerosol absorption, information about aerosol altitude needed.

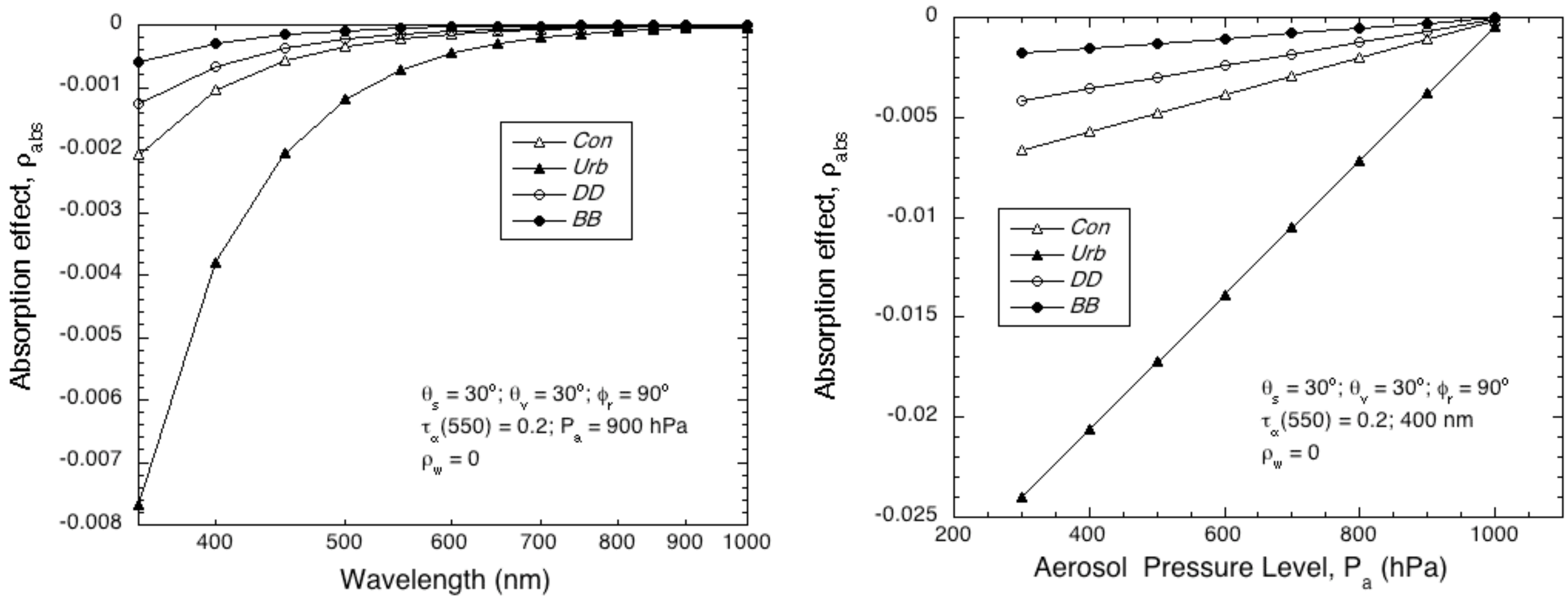

Absorption effect as a function of wavelength (top left), air mass (bottom left), and aerosol pressure level (top right) for continental, urban, desert dust, and biomass burning aerosol models. The effect increases in magnitude with decreasing wavelength, decreasing aerosol pressure level, and increasing air mass.

-Coupling between molecule and aerosol scattering depends on aerosol altitude, even when aerosols are not absorbing.

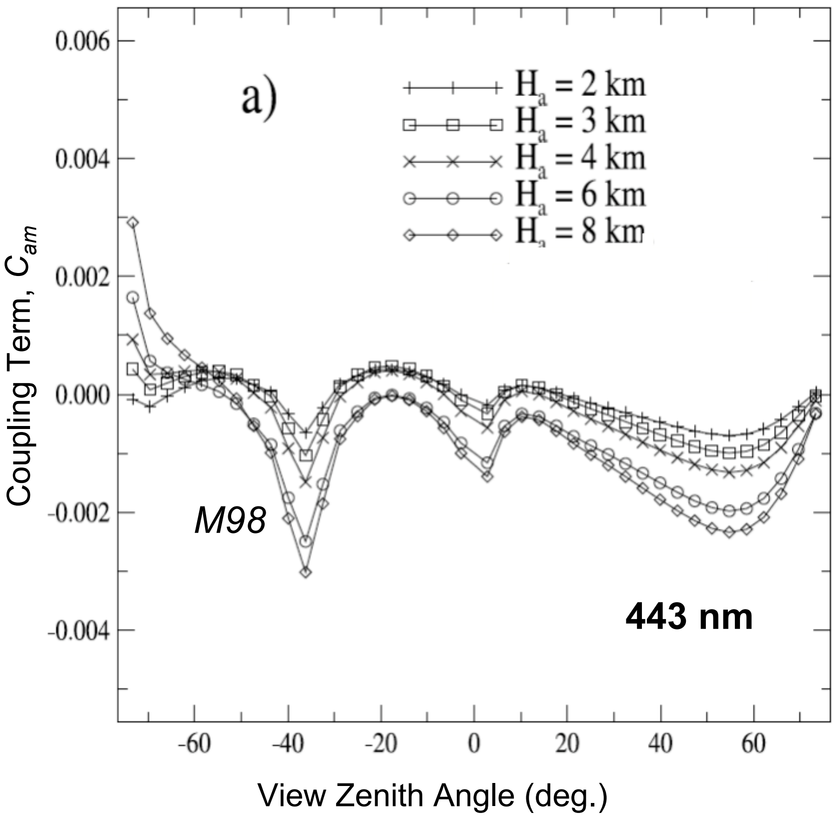

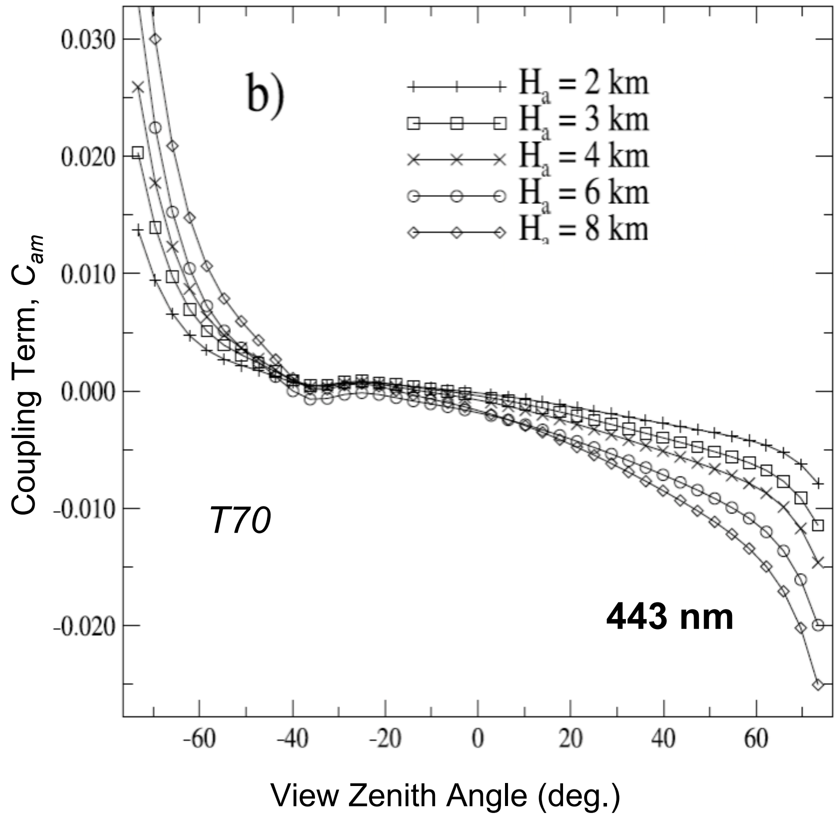

Effect of aerosol altitude, H_a, on the coupling term, C_{am}, of the atmospheric reflectance due to interactions between aerosol and molecular scattering. Wavelength is 443 nm and aerosol models are M98 (a) and T70 (b). Aerosol optical thickness is 0.1 at 865 nm. Solar zenith angle is 36.2 degrees. Results are for the principal plane (negative zenith angles correspond to backscattering). The case of H_a = 8 km corresponds to homogeneously mixed aerosols and molecules. (Adapted from Thieuleux, 2002.)

3. Determining separately the governing aerosol properties, i.e., single scattering albedo, phase function, optical thickness, and vertical distribution, using state-of-the art algorithms, may not allow sufficiently accurate atmospheric correction.

-State-of-the art retrieval errors on aerosol parameters:

•Hasekamp et al. (2011), multi-angle photopolarimetry:

$0.1 < \tau_a(550) < 0.3$

$\Delta r_f = 0.036$; $\Delta r_c = 0.24$ (micron)
$\Delta \sigma_f = 0.071$; $\Delta \sigma_c = 0.30$
$\Delta m_{rf} = 0.055$; $\Delta m_{rc} = 0.016$;
$\Delta m_{if} = 0.018$; $\Delta m_{ic} = 0.02$

$\Delta \tau_a = 0.024$
$\Delta \omega_a = 0.02\text{-}0.05$
$\Delta P_a = 5\text{-}10\%$

•Dubuisson et al. (2007), oxygen A-band technique:

$\Delta H_a = 1\text{-}2$ km ($\Delta p_a = 100\text{-}200$ hPa)

Retrieval errors are generally too large to meet the 5% accuracy requirement for water-leaving radiance.

Accuracy requirements on aerosol parameters, to achieve separately 5% error on water-leaving radiance at 450 nm, clear and turbid waters. Sun and view zenith angles are 30°, and relative azimuth angle is 90°.

Aerosol Model	λ = 450 nm, *[Chl]* = 0.06 mg/m^3			
	$\Delta\tau_a$	$\Delta\omega_a$	ΔP_a	Δp_a (hPa)
Maritime	±0.024	---	±0.016	>1000
Continental	±0.020	±0.040	±0.014	±214
Urban	±0.024	±0.028	±0.016	±51
Desert Dust	±0.022	±0.052	±0.017	±344

Aerosol Model	λ = 450 nm, *[Chl]* = 2.34 mg/m^3			
	$\Delta\tau_a$	$\Delta\omega_a$	ΔP_a	Δp_a (hPa)
Maritime	±0.006	---	±0.002	±308
Continental	±0.002	±0.005	±0.002	±27
Urban	±0.003	±0.004	±0.002	±6
Desert Dust	±0.003	±0.006	±0.002	±43

-Consequences:

•Retrieving individual aerosol parameters may not be adequate strategy for atmospheric correction. One needs to consider/ estimate the aerosol signal more directly.

•Aerosol information will be helpful to constrain the solution to the inherently ill-posed inverse problem in determining the aerosol radiance.

4. Accuracy requirements for atmospheric correction depend on the algorithm used to retrieve water-body variables.

-Reflectance ratio (RR) algorithm:

$(R_w)_{obs} = (R_w)_{true} + \delta R_w$

$RR_{obs} = RR_{true} [1 + \delta R_w(\lambda_1)/R_w (\lambda_1)]/[1 + \delta R_w(\lambda_2)/R_w (\lambda_2)]$

Large δR_w errors are acceptable as long as

$\delta R_w(\lambda_2)/R_w (\lambda_2) \approx \delta R_w(\lambda_1)/R_w (\lambda_1)]$

-GSM algorithm

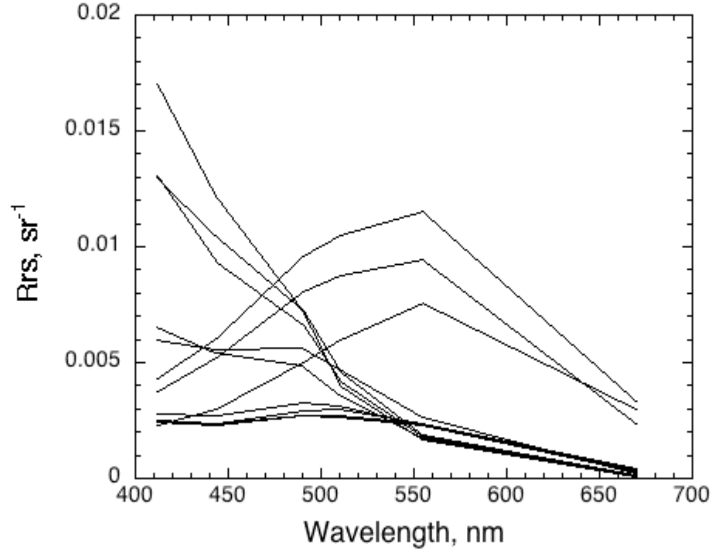

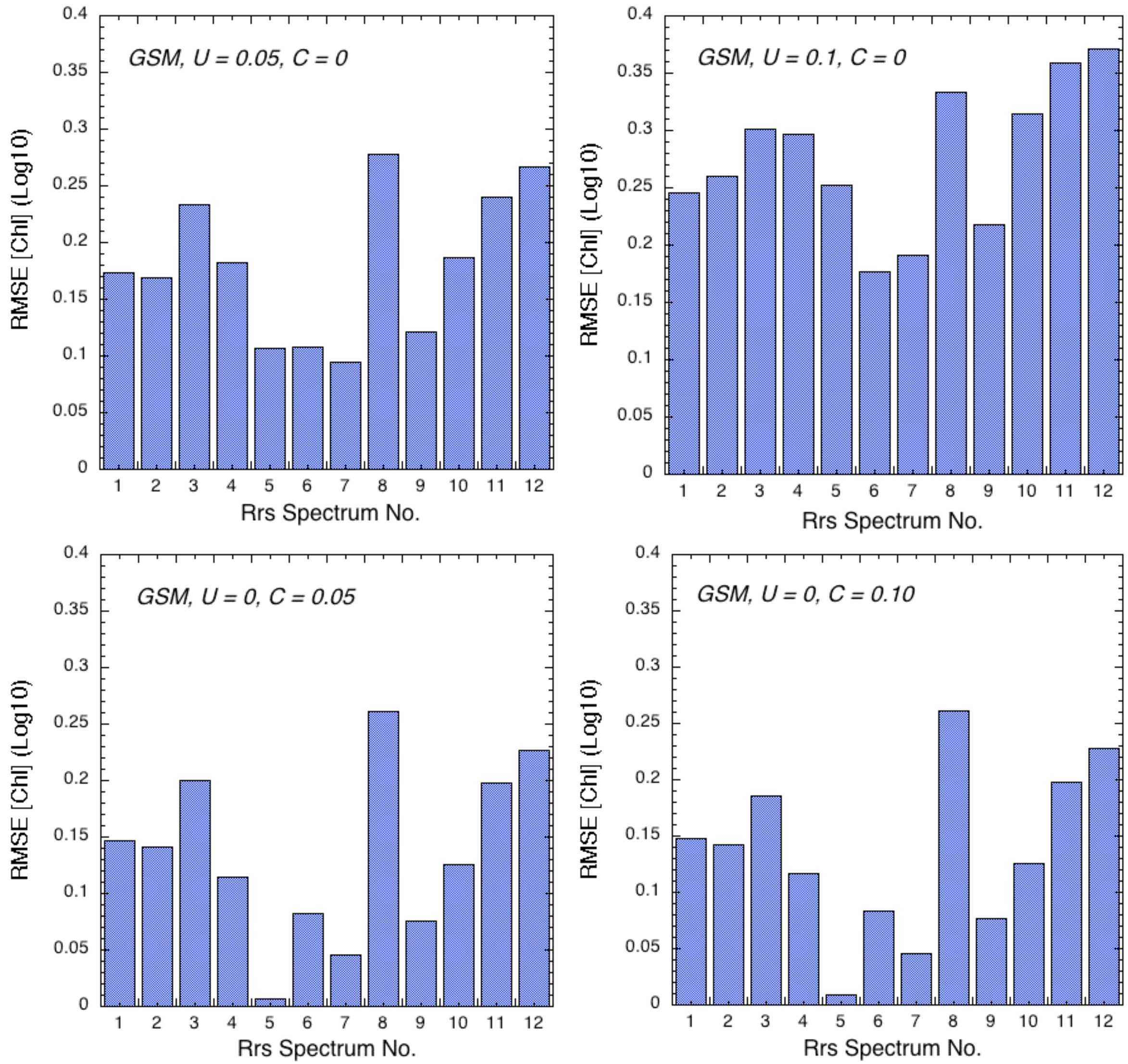

Noise Cases:

1) U = 0.05, C = 0

2) U = 0.10, C = 0

3) U = 0, C = 0.05

4) U = 0, C = 0.10

1000 Rrs realizations for each case

Impact of Rrs errors on GSM [Chl] retrieval. $Rrs_n(\lambda) = Rrs_0(\lambda)*(1 + U*e_u(\lambda) + C*e_c)$, where U and C are noise amplitudes, uncorrelated and correlated spectrally, and e_u and e_c are random numbers with a mean zero and a variance of unity.(Courtesy of S. Maritorena.)

5. Perturbing signal from the atmosphere and surface, even though resulting from complex processes and interactions, therefore difficult to model accurately, is smooth spectrally.

-Representation by a polynomial or a linear combination of orthogonal components with a few terms or eigenvectors is accurate: $\rho_p(\lambda_i) \approx \Sigma_j\, [a_j \lambda_i^{n_j}]$ or $\rho_p(\lambda_i) \approx \Sigma_j\, [c_j e_{ji}]$.

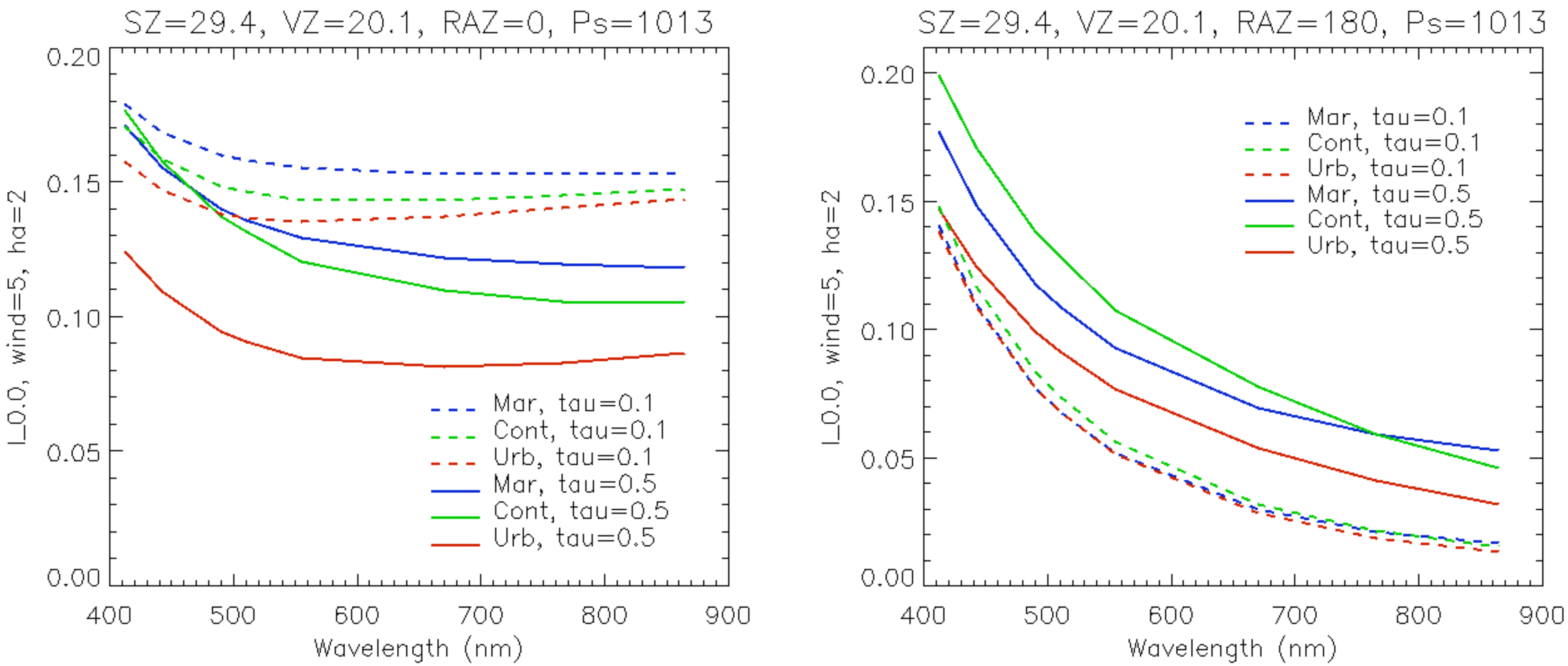

Simulations, using a successive-orders-of-scattering code, of the top-of-atmosphere normalized radiance in the solar plane for several aerosol conditions. Water body is black. (Left) Forward scattering. (Right) Backscattering.

Atmospheric Correction in the Presence of Sun glint and Thin Clouds

1. Introduction

-In the state-of-the-art operational atmospheric correction algorithms, the presence of a cloud or even a minimum amount of Sun glint definitely prevents utilization of the data.

-Consequently, the daily ocean coverage is typically 15-20%, and weekly products show no information in many areas.

-This limits considerably the utility of satellite ocean color observations in oceanography. Global coverage is required every three to five days in the open ocean and at least every day in the coastal zone.

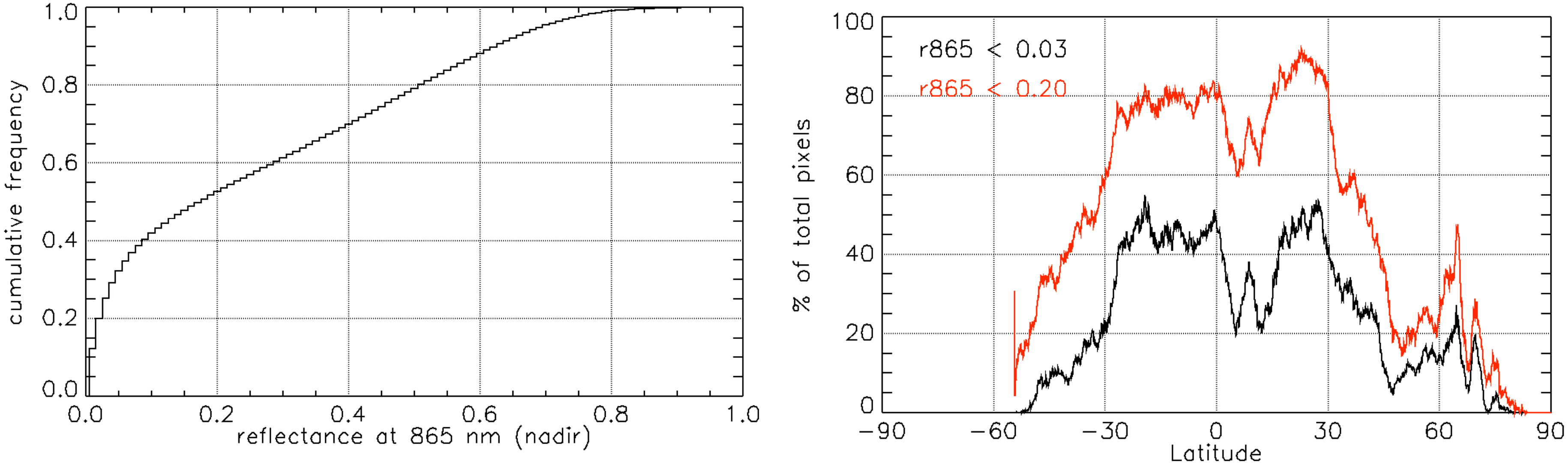

Left: Cumulative histogram of the top-of-atmosphere reflectance at "nadir" observed by POLDER-2 over the global ocean on 02 July 2003. Here "nadir" refers to the direction of observation closest to nadir. Right: Percentage of POLDER-2 pixels (observations of 02 July 2003) selected by a threshold of 0.03 and 0.2 for the "nadir" reflectance at 865 nm. (Courtesy of J.-M. Nicolas.)

2. Methods

-Spectral optimization (POLYMER), Steinmetz et al.

-PCA-Based atmospheric correction, Gross et al.

•Forward/inverse neural Networks, Doerffer et al.

POLYMER Algorithm

-Originally developed to process MERIS data in glitter-affected areas.

-Does not use a specific aerosol model, but fits the atmospheric reflectance by a polynomial with

(a) a non-spectral term that accounts for any non-spectral scattering (*clouds, aerosol coarse mode*) or reflection (*glitter, whitecaps, small ice surfaces*),

(b) a spectral term with a power law in λ^{-1} (*fine aerosol mode*), and

(c) a spectral term with a power law in λ^{-4} (*adjacency effects from clouds and white surfaces*).

$$\rho_{gam} = \rho_p - \rho_m = C_0 + C_1 \lambda^{-1} + C_2 \lambda^{-4}$$

-Marine reflectance is parameterized as a function [*Chl*] and a backscattering coefficient for non-phytoplankton particles, B_{bs}.

-The five parameters C_0, C_1, C_2, *Chl*, and B_{bs} are determined by minimizing the difference between observed and modeled reflectance.

-Example of MERIS data processing by the POLYMER algorithm

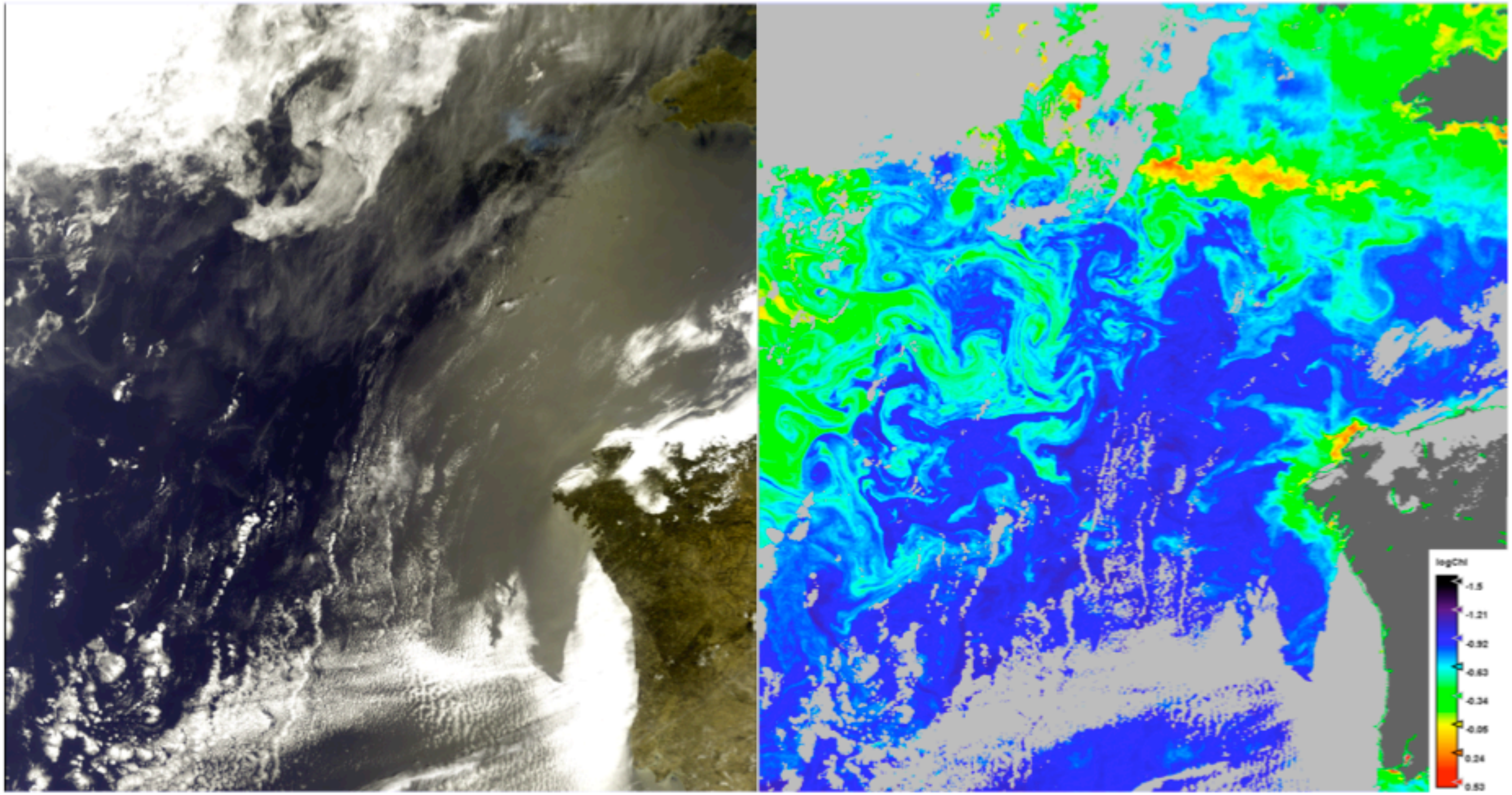

RGB composite of a MERIS scene off Portugal, 21 June 2005 (left) and chlorophyll concentration derived by the POLYMER algorithm (right). Chlorophyll concentration is retrieved in the presence of thin clouds and sun glint, and the chlorophyll patterns exhibit spatial continuity from cloud- and glint-free areas to adjacent cloud- and/or glint-contaminated areas. (Courtesy of F. Steinmetz.)

-Increase in daily spatial coverage by the POLYMER algorithm

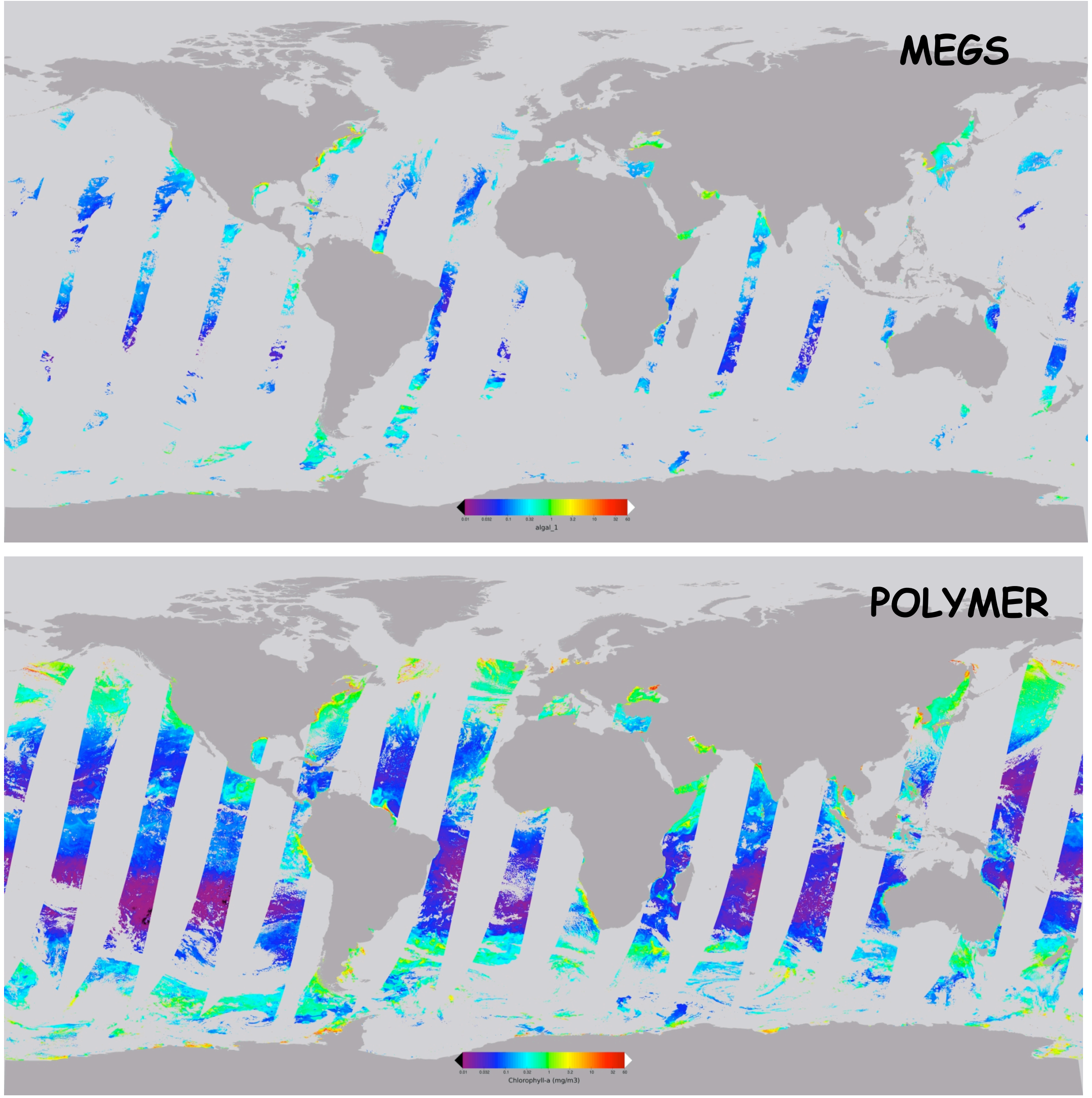

MERIS level 2 imagery of chlorophyll concentration, 21 December 2003.

-Increase in spatial coverage by the POLYMER algorithm, 3-day composite

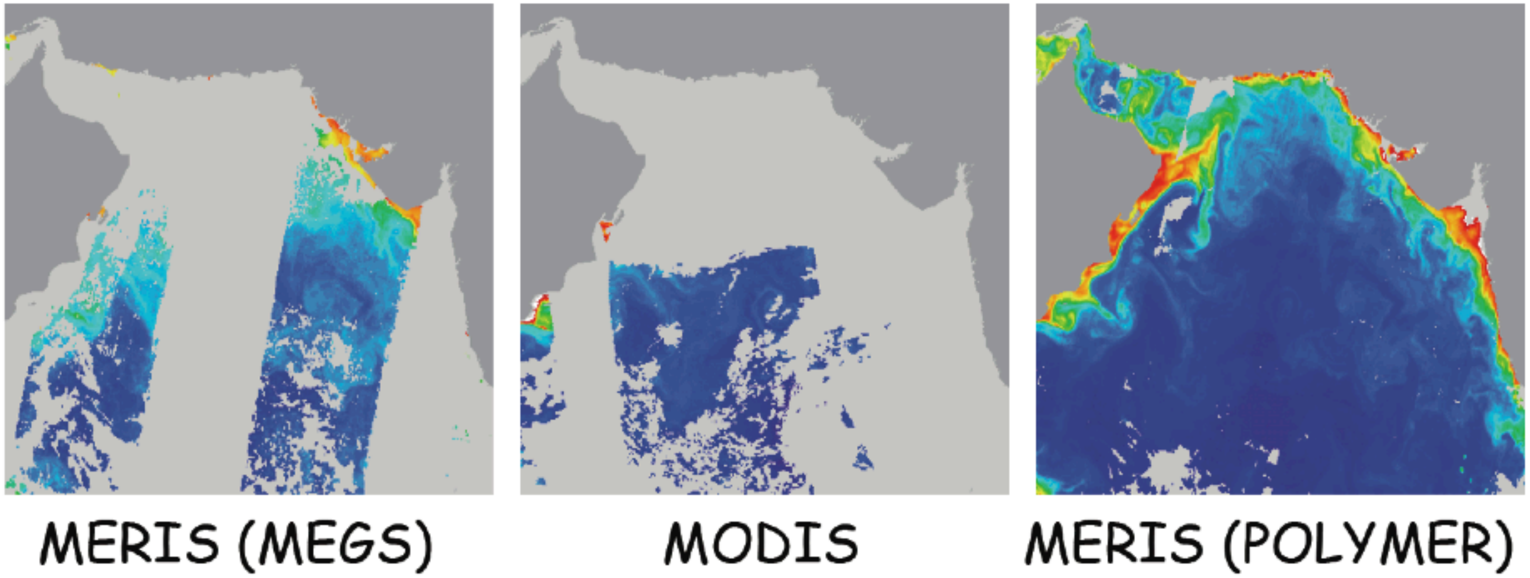

Level 3 composites of chlorophyll concentration, 3 to 5 June 2003, in the Arabian Sea, showing a dramatic increase in spatial coverage by the POLYMER algorithm.

-Evaluation of POLYMER algorithm using MERMAID data set

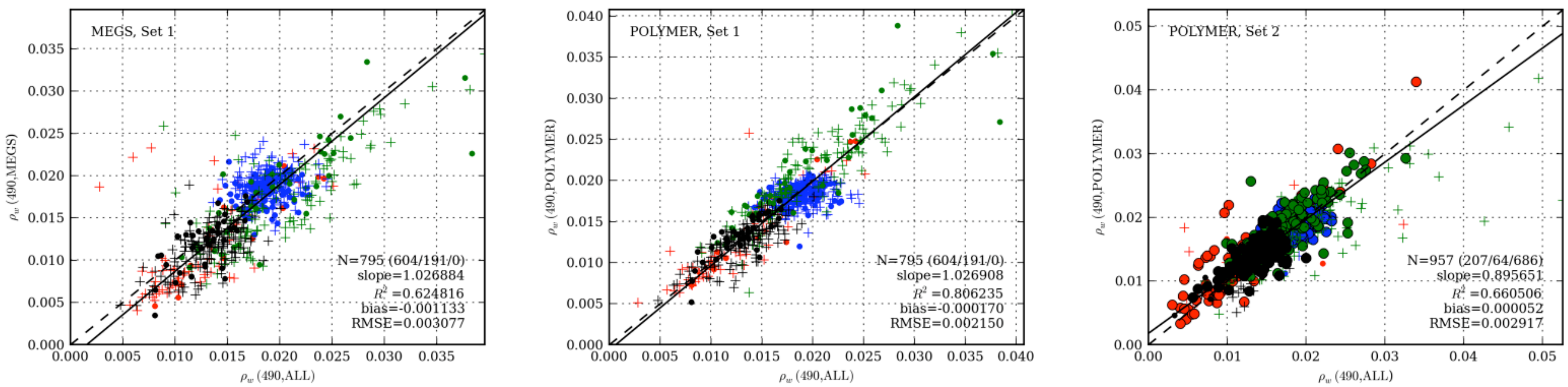

Scatter plots of marine reflectance at 490 nm derived from MERIS, for the standard MEGS processing (left) and the POLYMER processing (middle and right). The match-up Set 1, left and middle (795 points), is common to MEGS and POLYMER processing and does not include match-ups contaminated by glitter and thin clouds. Flags for clouds and glitter have been relaxed in match-up Set 2 for POLYMER (957 points).

PCA-Based Algorithm

-TOA reflectance (after correction for molecular scattering effects) is decomposed in principal components.

-Components sensitive to the ocean signal are selected and combined to retrieve the principal components of marine reflectance, allowing reconstruction of the marine reflectance.

$$\rho = \rho_{TOA} - \rho_m = f(\rho_w)$$

$$\rho = \Sigma_i \, c_{pi} \mathbf{e}_{pi}$$

$$\rho_w = \Sigma_j \, c_{wj} \mathbf{e}_{wj}$$

$$c_{wj} = g(c_{pi}\text{'s})$$

-PCA-Based retrieval, Arabian Sea

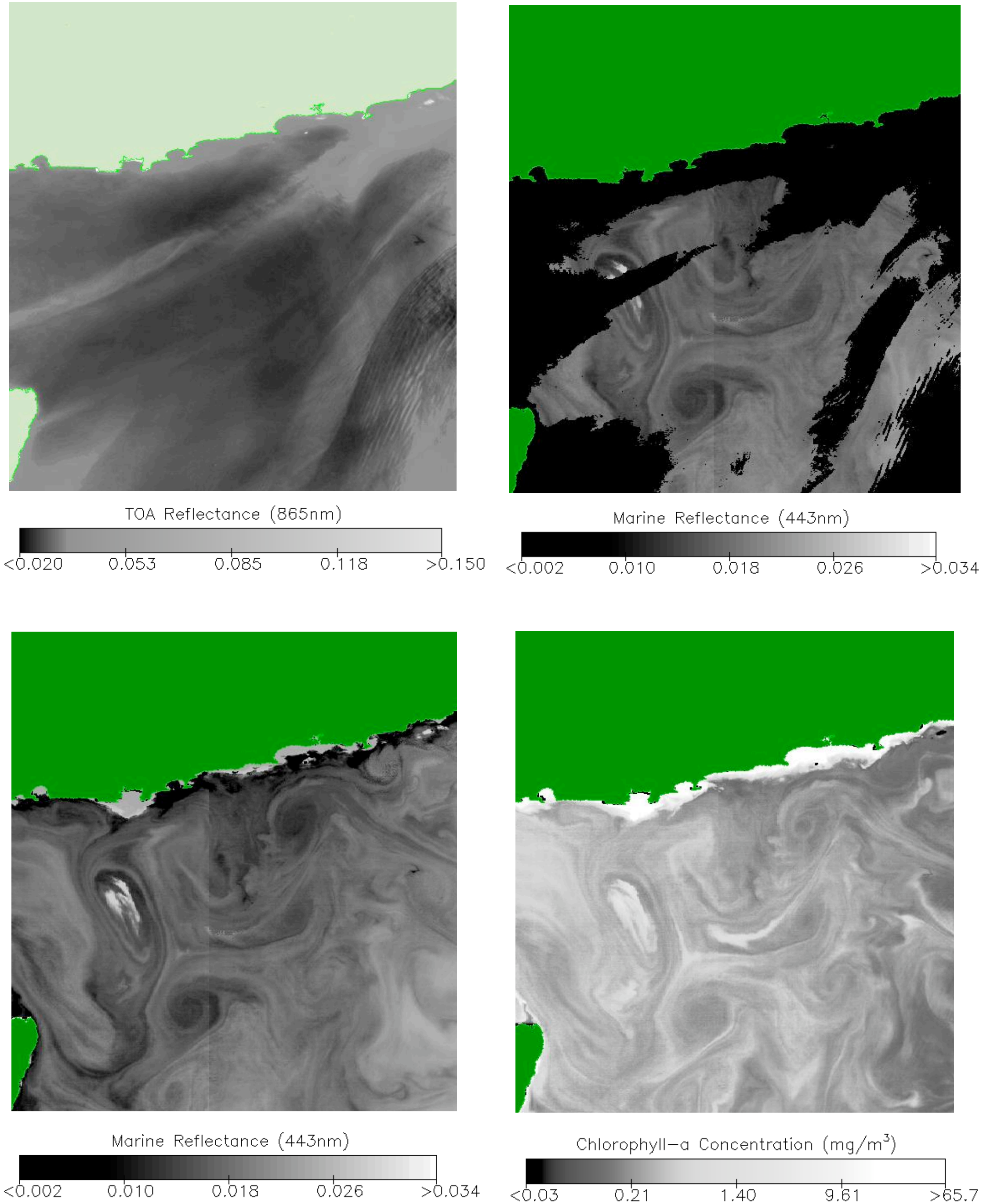

Imagery acquired by MERIS over the Arabian Sea on 09 November 2003. Top left: Reflectance at 865 nm showing thin clouds. Top right: Retrieved marine reflectance (PCA-based algorithm) with threshold of 0.03 at 865 nm. Bottom left: Same as upper right, but threshold of 0.2 at 865 nm. Bottom right: Retrieved chlorophyll-a concentration with threshold of 0.2 at 865 nm.

PCA-based retrieval, Northeast Atlantic

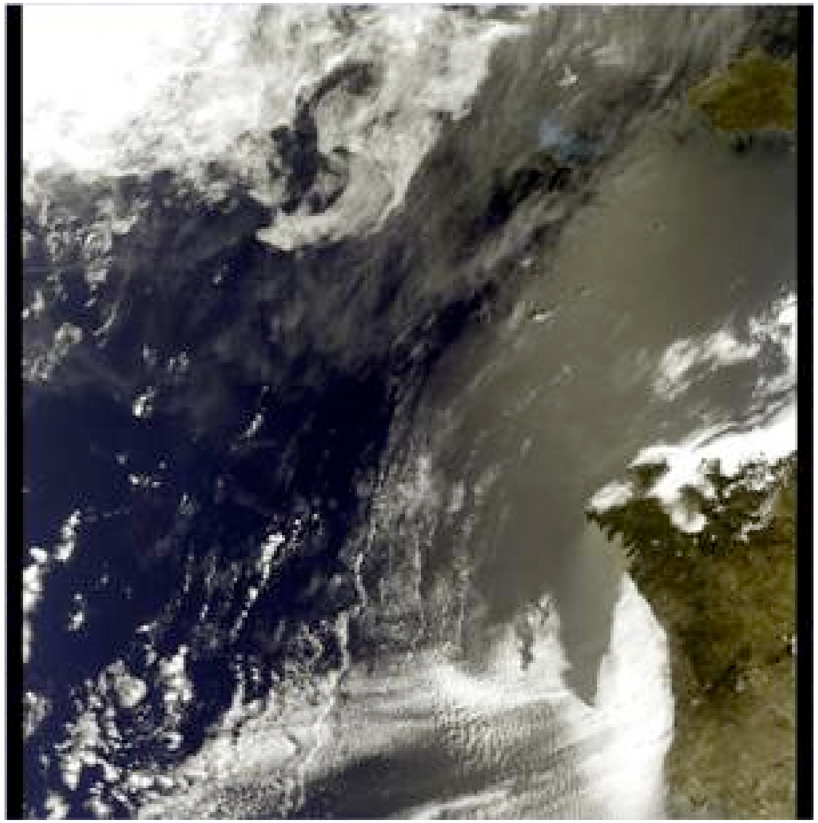

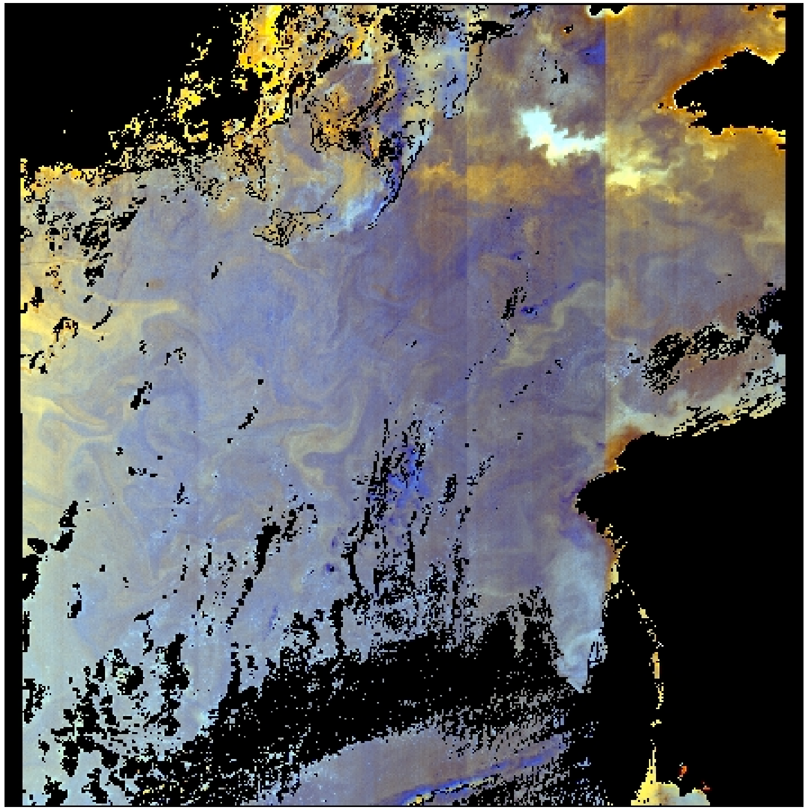

(Left) RGB composite of MERIS imagery off the coast of France and Portugal, 21 June 2005. (Right) RGB composite of marine reflectance retrieved by the PCA algorithm. Marine reflectance is retrieved in the presence of thin clouds and sun glint.

-PCA-Based retrieval, Black Sea

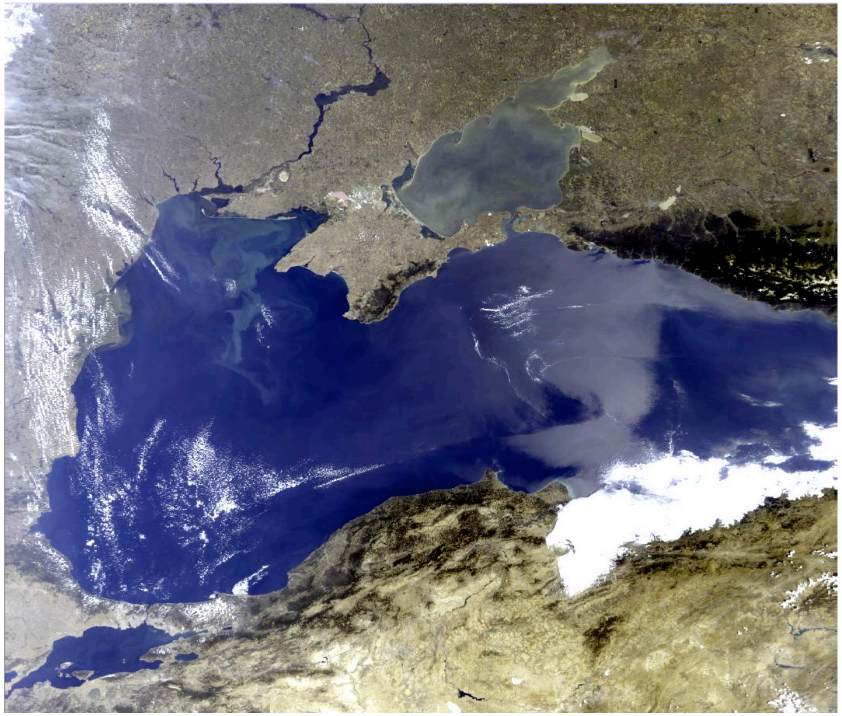

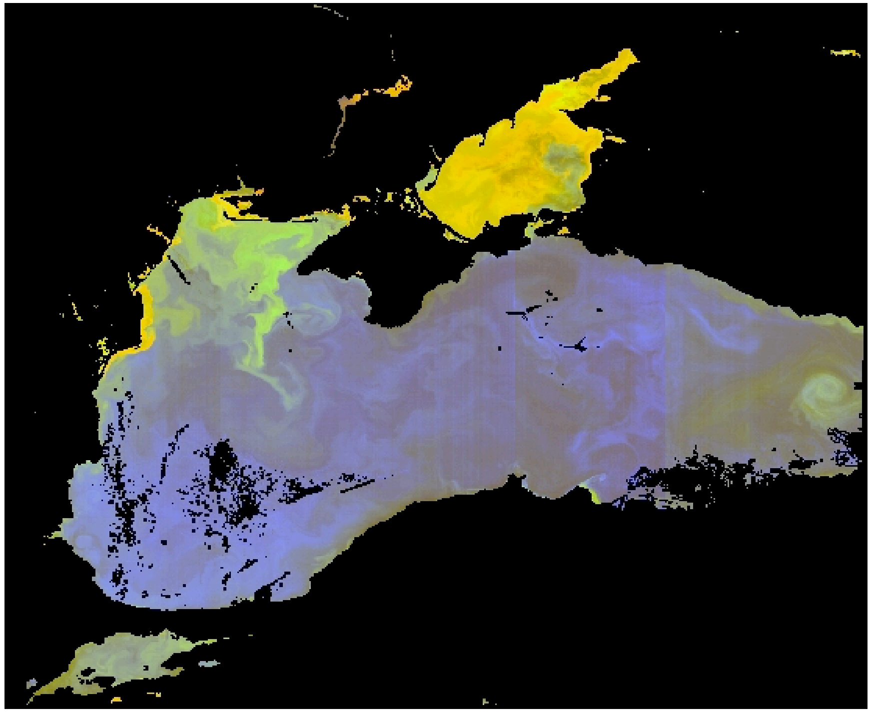

(Left) RGB composite of MERIS imagery of the Black Sea and Sea of Azov, 9 August 2008. (Right) RGB composite of marine reflectance retrieved by the PCA algorithm. Marine reflectance is retrieved in the presence of thin clouds and sun glint.

Neural Network Algorithm

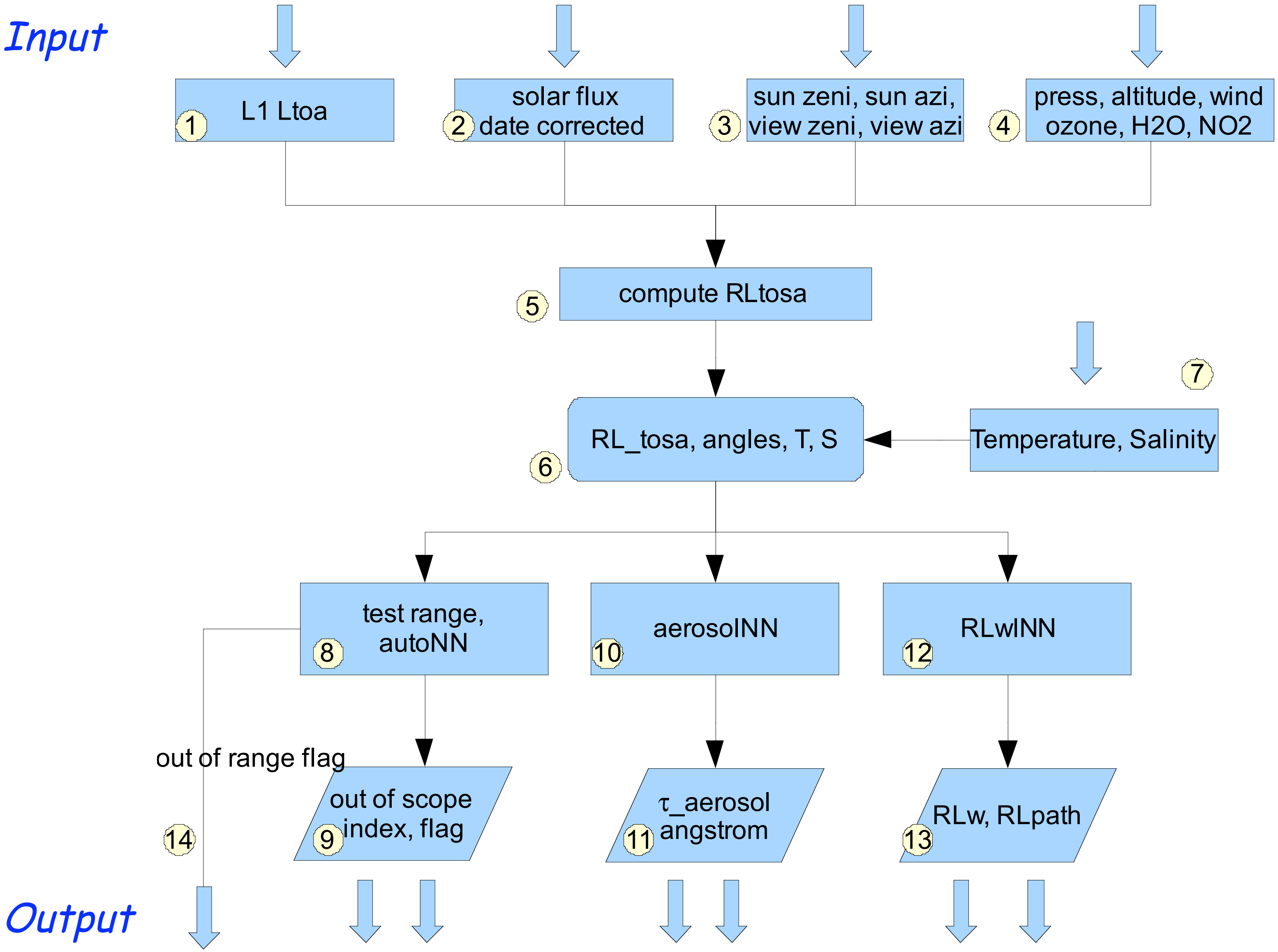

Schematic diagram of atmospheric correction using neural networks.

-NN-based retrieval, Baltic Sea and North Sea

RGB composite, TOA

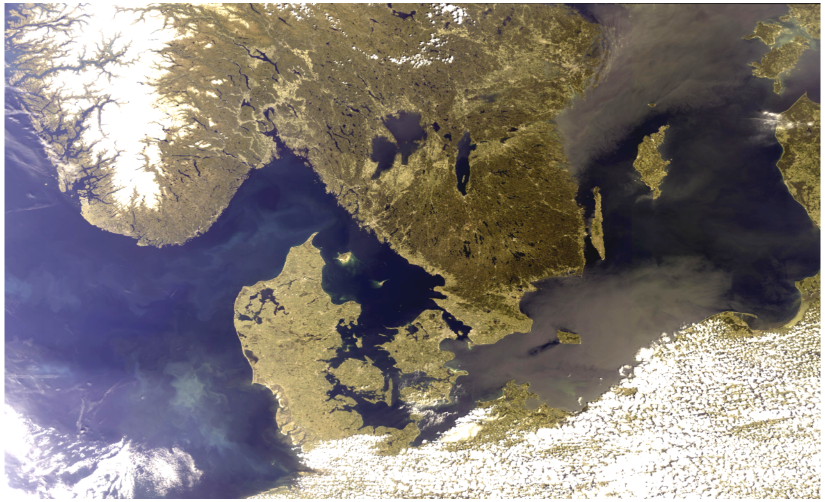

Path reflectance, 560 nm

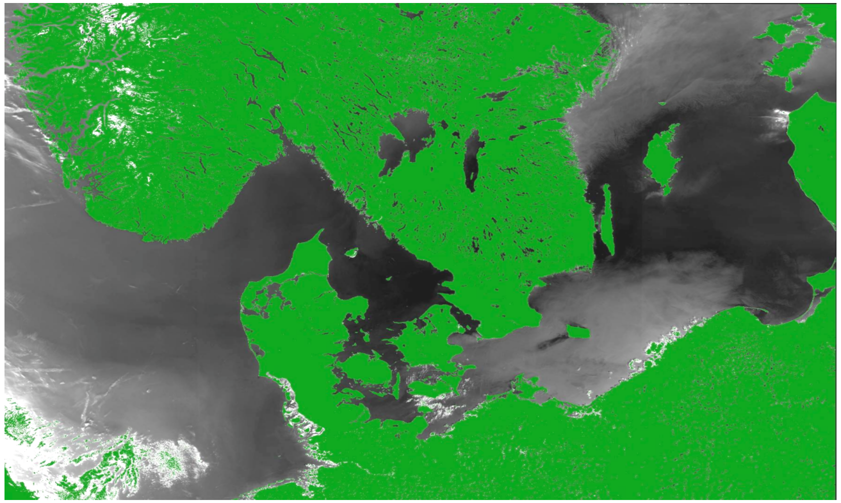

Water reflectance, 560 nm

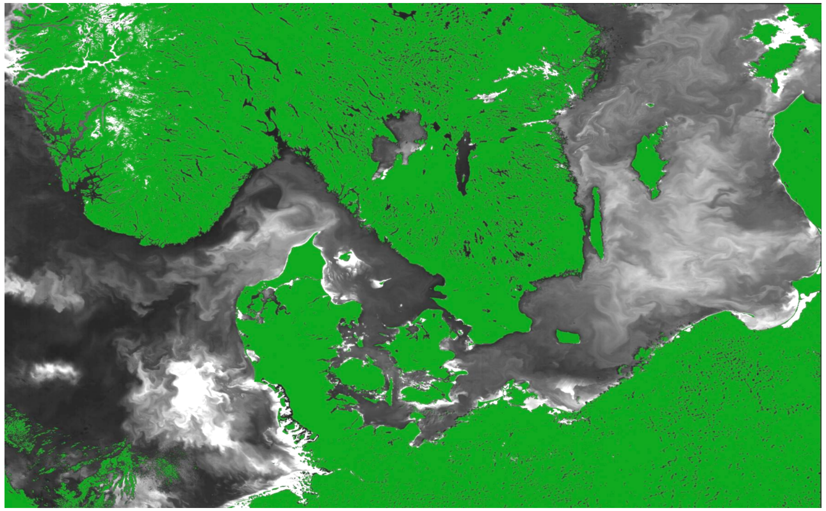

(Top Left) RGB composite of MERIS imagery of the Baltic and North Seas, 06 June 2006. (Top Right) Retrieved path radiance at 565 nm by the NN algorithm. (Bottom Left) Retrieved water reflectance at 565 nm by the NN algorithm.

-Evaluation of NN algorithm at MOBY site

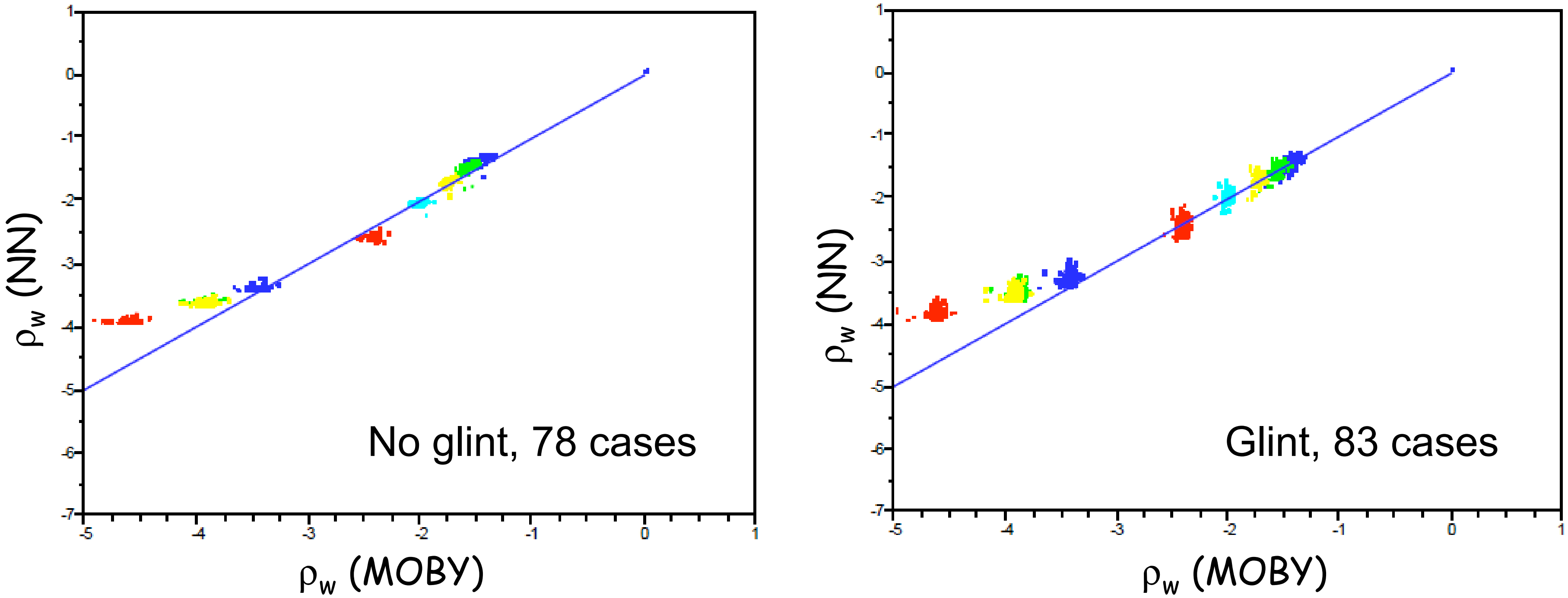

Scatter plots of MERIS-derived (NN algorithm) versus measured water reflectance at the MOBY site. Left: 78 cases with no glint. Right: 83 cases with glint.

Correction of Adjacency Effects

1. Definition/Importance

-Adjacency effects are associated with the change in digital number of a pixel caused by atmospheric scattering of radiance that originates outside of the sensor element's field of view.

-They are important in the coastal zone, or in the vicinity of clouds and sea ice, or even in the open ocean (e.g., upwelling systems), i.e., when the spatial contrast between the target and its environment is relatively large.

-They may affect significantly the retrieval of marine reflectance and chlorophyll concentration, all the more as pixel size is small. Scale of influence is larger for molecular scattering (12 km) than aerosol scattering (1 km), and when aerosols are located at a higher altitude.

-Adjacency effects are generally ignored in standard atmospheric correction schemes and operational processing of satellite ocean-color imagery.

2. TOA Adjacency Effect

-TOA reflectance, homogeneous surface:

$$R_t \approx R_a + R_w T_a(\theta_s) T_a(\theta_v)/(1 - R_w S_a)$$

-TOA reflectance, heterogeneous surface:

$$R_t^* \approx R_a + T_a(\theta_s)[R_w exp(-\tau_a/cos(\theta_v)) + R_e t_a(\theta_v)]/(1 - R_e S_a)$$

-Adjacency effect:

$$\Delta R_t = R_t^* - R_t \approx (R_e - R_w) t_a(\theta_v) T_a(\theta_s)$$

$$R_e = \int_{-\infty}^{+\infty} \int_{-\infty}^{+\infty} R_w(x,y) F(x,y) dxdy$$

F(x,y) : Atmospheric spread function.

-Example of TOA Adjacency Effect

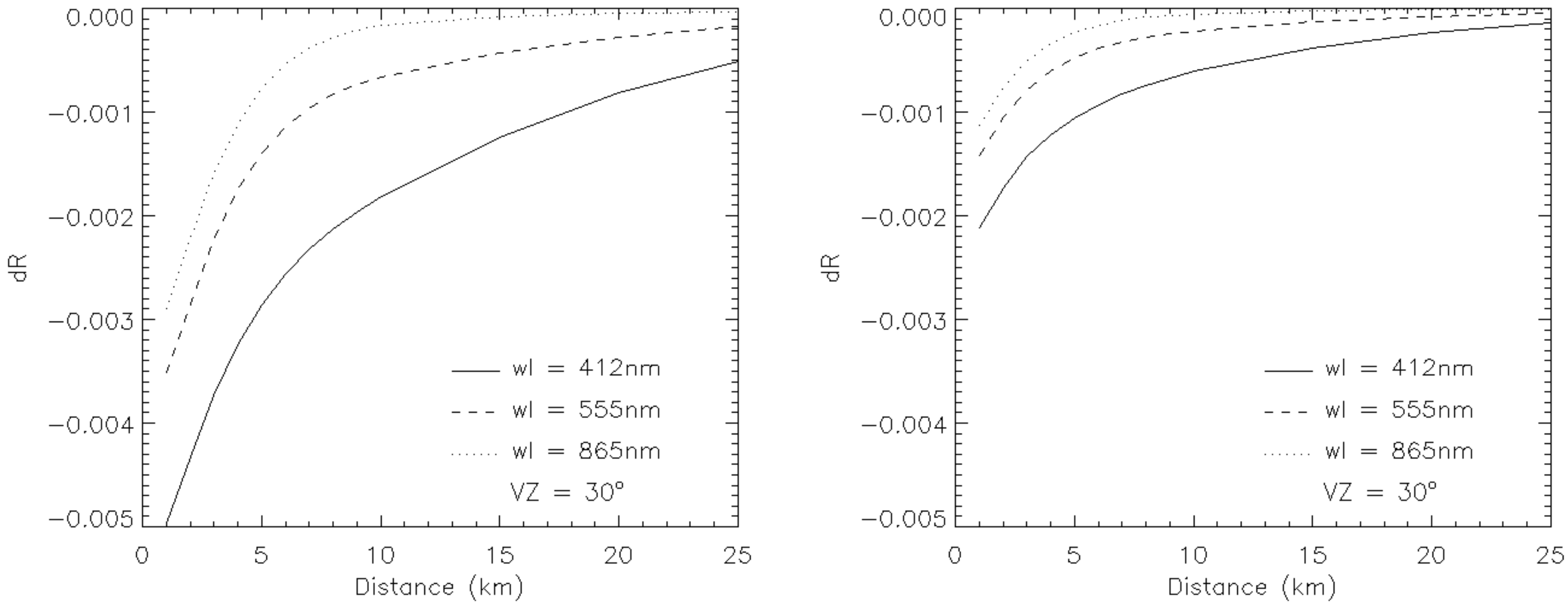

TOA adjacency effect, dR, as a function of distance for selected wavelengths. Aerosol optical thickness is 0.2. Solar and viewing zenith angles are 30 degrees. Left: The target is at the center of a circle of reflectance 0.03 surrounded by an environment of reflectance 0.01. Distance is the radius of the circle. Right: The target is in one side of a coastline separating regions of reflectance 0.03 (including the target) and 0.01. Distance is the shortest distance of the target to the coastline.

3. Correction of Adjacency Effect

-To correct the Level 1b imagery, one may apply a classic de-convolution algorithm and iterate, since reflectance of neighboring pixels is affected by the adjacency effect.

-This would allow the processing of Level 2 products assuming that the surface is homogeneous, i.e., using the large target formalism of the standard atmospheric correction scheme.

-An alternative is to apply the atmospheric algorithm to the original Level 1b imagery, use the derived marine reflectance and aerosol properties to compute ΔR_t, correct the TOA reflectance, and apply again the atmospheric algorithm to the corrected TOA reflectance.

-Example using SeaWiFS imagery (open ocean)

L_{TOA}(443 nm)

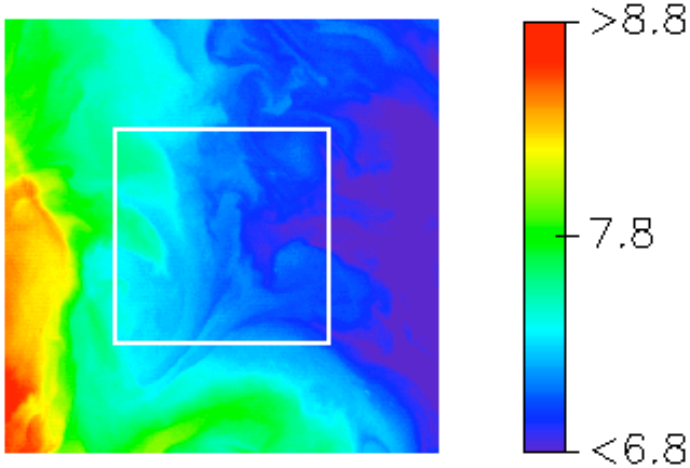

L_{TOA}(555 nm)

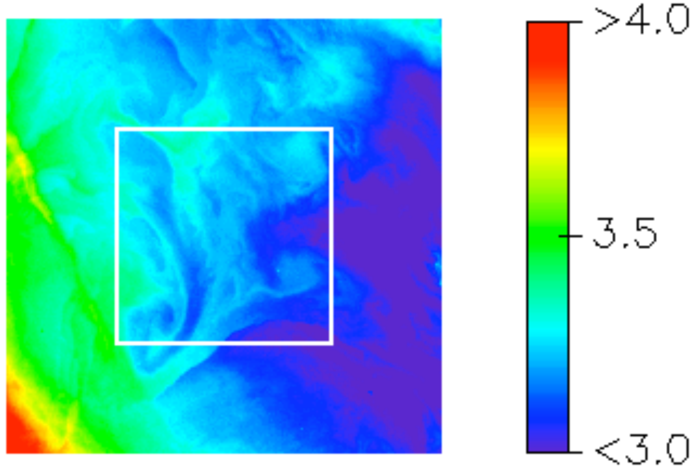

SeaWiFS LAC images of TOA Level 1b radiance at 443 and 555 nm ($mW/cm^2/\mu m/sr$) obtained on February 14, 1999 in upwelling region off the coast of Namibia. The image is about 200x200 km in size. White rectangle denotes area within which adjacency effects are estimated. De-convolution of spectral bands used for ocean color, i.e., 443 and 555 nm, was performed using the marine reflectance and aerosol content derived from the operational atmospheric correction algorithm.

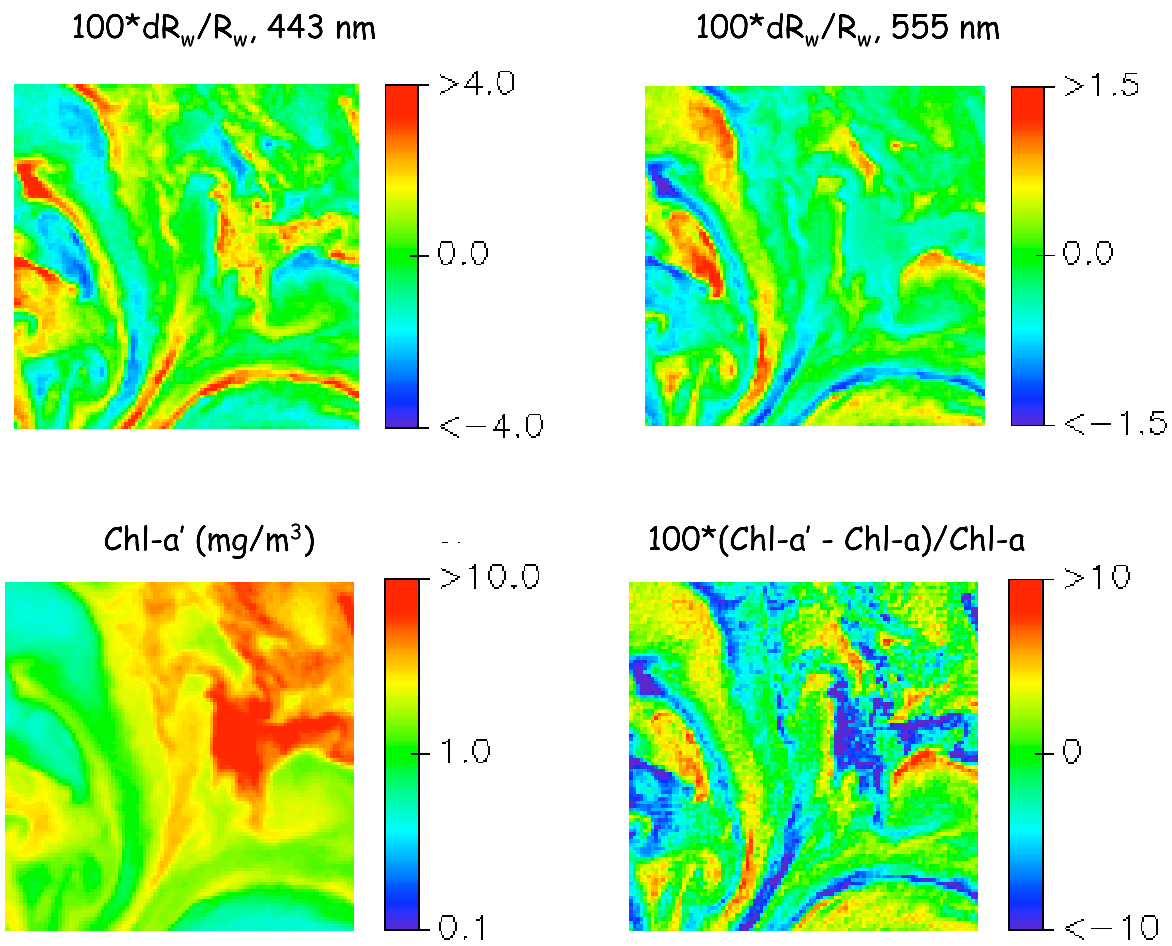

(Top left and top right) Error on marine reflectance at 443 nm and 555 nm due to adjacency effects. (Bottom left) Chlorophyll-a concentration computed from marine reflectance at 443 and 555 nm, with no correction for adjacency effects. (Bottom right) Error on chlorophyll-a concentration due to adjacency effects.

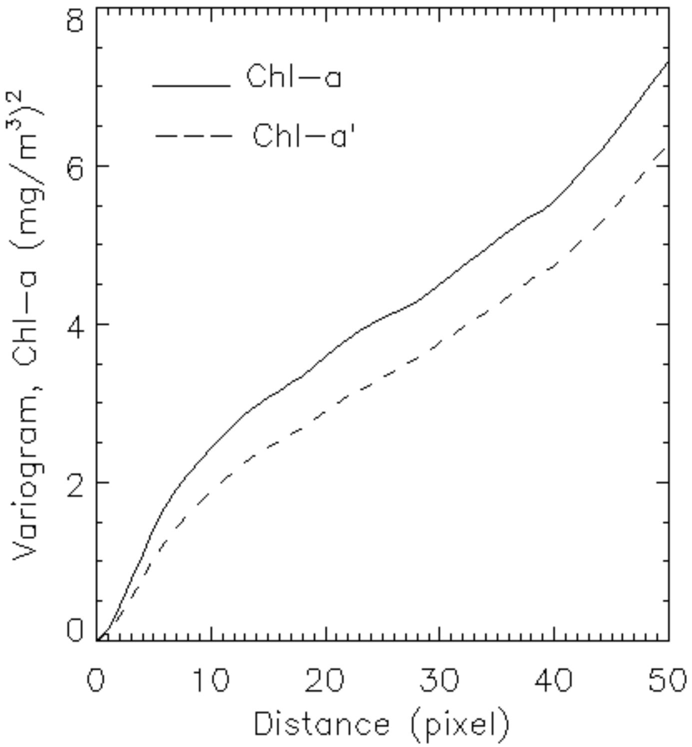

Variogram of chlorophyll concentration. Spatial correlation is changed significantly (spatial dependence between observations is decreased after correction of adjacency effects, suggesting more influence of local processes).

-Another way to deal with adjacency effects is to use/ develop atmospheric correction algorithms that reduce the effects. This is expected from algorithms that use all available spectral information.

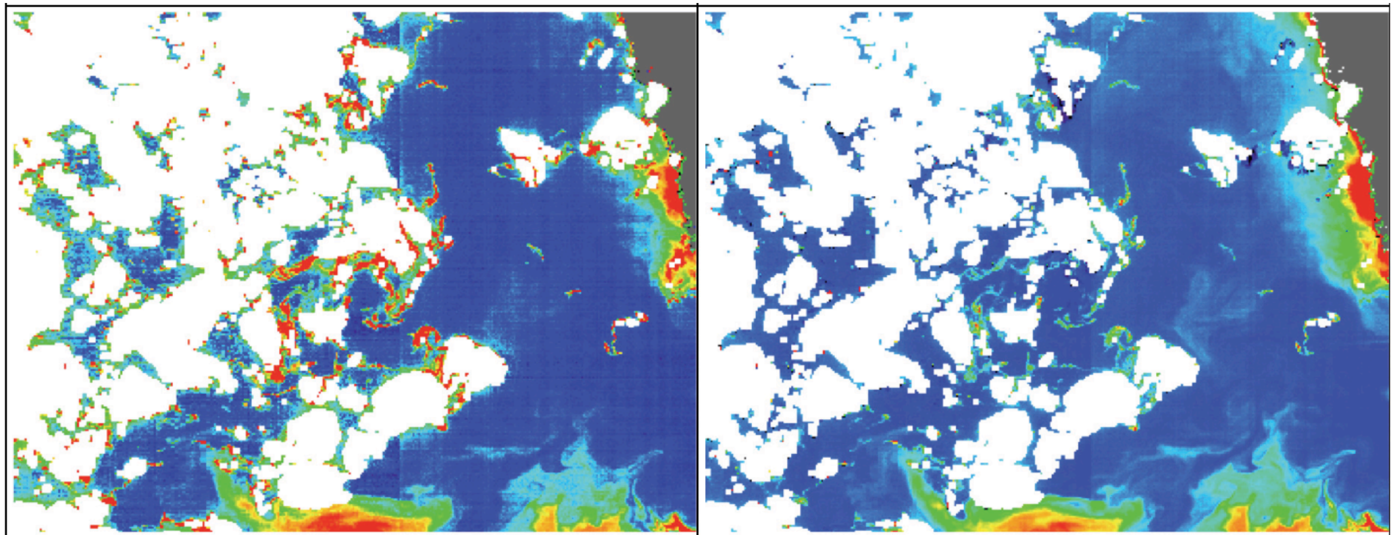

Water reflectance at 560 nm, MEGS processing (detail)	Water reflectance at 560 nm, POLYMER processing (detail)
Beaufort Sea, 2008-07-04, MERIS	

MERIS image of the Beaufort Sea showing that the standard processing is affected by the ice environment, leading to an anomalous increase of retrieved reflectance at 560 nm (left). Adjacency effects are reduced with the POLYMER algorithm.

Conclusions

-Atmospheric correction of satellite ocean-color imagery can be performed through thin clouds and in the presence of Sun glint, and in the vicinity of clouds, sea ice, and land.

-The POLYMER, PCA-based, and NN algorithms yield imagery that is comparable with standard imagery. Spatial continuity is good from cloud- and glint-free areas to adjacent cloudy and/or glint-affected areas, and values are more realistic near sea ice.

-The daily ocean coverage, 15-20% with standard algorithms, is expected to increase substantially with the POLYMER, PCA-based, and NN algorithms (by up to 50%?).

-The gain in coverage will allow one to resolve better phytoplankton blooms in the open ocean and, for example, "events" linked to wind forcing in the coastal zone. This could lead to important new information about the temporal variability of biological processes.